JOURNAL OF MATERIALS SCIENCE 13 (1978) 1671-1679

X-ray diffraction line profile analysis of diffusional homogenization in powder blends

R. DELHEZ, E. J. MITTEMEIJER, E. A. van den BERGEN
Laboratory of Metallurgy, Delft University of Technology, Rotterdamseweg 137, Delft, The Netherlands

A new nondestructive method – based on computer simulation of X-ray diffraction line profiles – is proposed to characterize homogenization in compacted binary powder blends. As a parameter to characterize the stage of homogenization the relative peak position is proposed. This parameter is easy to determine in practice: during homogenization the position of an X-ray diffraction maximum is traced. As compared to other methods the present one has the following advantages: (i) it is fast and simple and (ii) it allows a more severe test of the model of interdiffusion applied. Experiments were performed with compacted blends of copper and nickel powders at 800, 900 and 1000° C. At the start of homogenization diffusion was very fast. Experiments at lower temperatures revealed that this was due to surface diffusion at the contact places between the copper and nickel particles with an activation energy of about 12 kcal mol^{-1}. Because of the sensitivity of the relative peak position to the interdiffusion model adopted it was shown that the generally accepted concentric sphere model: nucleus of nickel and shell of copper, should be modified to include a pre-alloyed shell at the copper/nickel interface at $t = 0$. Then good correspondence between theory and experiment is obtained. Finally it was found that in the temperature range applied one diffusion mechanism is dominant with an activation energy of 32 kcal mol^{-1}, indicating grain boundary diffusion.

1. Introduction

The fabrication of alloys by diffusional homogenization of compacted powder blends is technologically important [1]. To control such processes characterization of the interdiffusion occurring in the powder blend is necessary. X-ray diffraction line profile analysis appears to be a powerful quantitative nondestructive method to determine concentration profiles: A concentration profile corresponds to a lattice parameter profile and – according to Bragg's law – a spectrum of lattice parameters causes line broadening.

In recent years attention has been paid to the development of the theory of diffraction from concentration profiles in monocrystalline systems [2, 3]. For powder specimens a method for the interpretation of line broadening resulting from binary interdiffusion was proposed by Rudman [4]. This technique has been applied on interdiffused blends of copper and nickel powders [1, 5, 6]. From these studies it appeared that a concentric sphere geometry may afford the best description of interdiffusion in compacts of blended metal powders: the minor component is represented by a spherical particle, the major component by a uniform shell around the sphere.

The purpose of this paper is to propose a new method to analyse interdiffusion in compacted powder blends. The method is based on computer simulations of the X-ray diffraction line profiles. A new parameter characterizing the stage of homogenization will be proposed: the relative peak position. The method has the following advantages:

(i) Simulations are simple and have to be done only once for a system;

(ii) The relative peak position is directly available from experiment and can be measured in a very short time. Thus diffusion processes may be followed *in situ*;

(iii) As compared to Rudman's "degree of interdiffusion" – which is obtained by an elaborate calculation – the relative peak position is more sensitive for the actual diffusion model.

Several results on the homogenization in blends of copper and nickel powders will be presented. Argument (iii) resulted in a modification of the usual concentric sphere model.

2. Experimental procedure

2. 1. Sample preparation

Commercially available pure powders were used: Nickel (Koch-Light; 8500 W; $\langle\phi\rangle \simeq 14\,\mu m$); Copper (Koch-Light; 8223 h; $\langle\phi\rangle \simeq 35\,\mu m$). The powders were reduced in a 98% Ar/2% H_2 atmosphere at 350 to 400° C during 1 h. No measurable sintering occurred. Portions of the powders, all with 30 at % Ni, were thoroughly mixed by tumbling together for about 12 h. The powder blends were cold pressed at $(8.28 \pm 0.02) \times 10^8\,N\,m^{-2}$. Discs were obtained with a diameter of about 13 mm and a thickness of about 2 mm.

The diffusion anneals were performed in a 98% Ar/2% H_2 atmosphere in a furnace controlled automatically to ±2° C. The temperatures used were 800, 900 and 1000° C. The annealing times were corrected for the time needed for the specimens to warm up [7]. After diffusion a surface layer (100 to 150 μm thick) was removed by grinding and mechanical polishing. The cold work thus induced was removed by an anneal at 500° C for 10 min. No interdiffusion occurred during this reheating.

2. 2. Diffractometry

Line profiles were measured in steps of 0.01° 2θ applying the preset-time method with a Siemens ω-diffractometer, equipped with a graphite monochromator. The 2 2 0 reflection was measured with CuKα radiation because (i) it is a good compromise between high intensity and angular (concentration) resolution and (ii) no overlap with neighbouring Kα and Kβ reflections occurs. Angle position corrections due to specimen transparency, flat specimen, 3° axial divergence (Soller slits were used) and specimen displacement were performed according to Wilson [8]. Background radiation was removed by linear interpolation. The α_2 component was eliminated according to Delhez and Mittemeijer [9], and the angular dependence of the Lorentz and polarization factors was corrected for according to the rules set out in [10]. The angular dependence of the structure factor F was taken into account as $F = xf_{Ni} + (1-x)f_{Cu}$, where x is the atomic fraction nickel. The angular dependencies of the atomic scattering factors f_{Ni} and f_{Cu} were obtained from [11].

3. Rudman's method

In this paper we intend to weigh the line profile simulation method (Sections 5 and 6) against the Rudman method [4]. We also slightly modified the Rudman technique. Therefore it is appropriate to sketch briefly our version of the Rudman analysis.

If particle size and strain broadening are neglected and s is given by $2 \sin\theta/\lambda$ ($= 1/d(x)$, where $d(x)$ is the interplanar spacing), the volume fraction $p(x)\partial x$ of compositions between x and $x + \partial x$ follows from (cf. [12]

$$p(x)\partial x = C_1 \frac{(-\partial d(x)/\partial x)v^2(x)}{d^2(x)} I(s)\partial x \qquad (1)$$

where C_1 is a constant (including the absorbtion factor which is approximately constant, $v(x)$ is the unit cell volume and $I(s)$ is the intensity corrected according to Section 2. 2. It should be pointed out that the previous investigators [1, 4–6] did not consider the concentration dependence of the unit cell volume. This implies that these authors did not correct for a 9% intensity lapse in the line profiles of their Cu/Ni powder specimens.

An effective penetration depth $y(x)$ is defined

$$y(x) = \int_0^x p(x)\partial x \qquad (2)$$

and then a plot of x versus y is analogous to normal concentration–penetration curves.

Rudman [4] proposed the degree of interdiffusion F as a parameter to characterize the stage of homogenization. F is defined by the ratio of the quantity of material which has crossed the Matano interface after a given diffusion time to the quantity of material which will cross in infinite time:

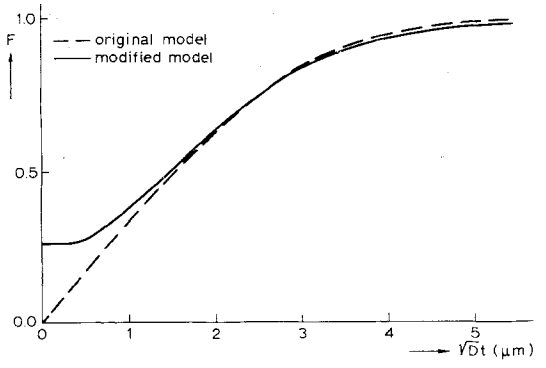

Figure 1 The dependence of the degree of interdiffusion F on Dt, where D is the diffusion coefficient and t the annealing time, according to the original concentric sphere model and the modified one (cf. Section 6.2).

$$F = \frac{\int_{x=0}^{x(y=y_M)} (y_M - y)dx + \int_{x(y=y_M)}^{x=1} (y - y_M)dx}{\bar{x}y_M + (1-y_M)(1-\bar{x})}$$

$$= \frac{2\int_{x=0}^{x(y=y_M)} (y_M - y)dx}{2\bar{x}y_M} \qquad (3)$$

where y_M represents the Matano interface and $\bar{x}$ the average composition of the sample. For the concentric sphere model the ratio F is calculated analytically in the Appendix (let $\Delta_1 \to 0$ and $\Delta_2 \to 0$ in Equation (A2)) in contrast with previous graphical integrations [5, 6]. The dependence of F on Dt, where D is the interdiffusion coefficient and t is the annealing time, is shown in Fig. 1. From the definition of F it is clear that this parameter is rather insensitive to considerable deviations from the concentric sphere model as will be illustrated in Section 6.

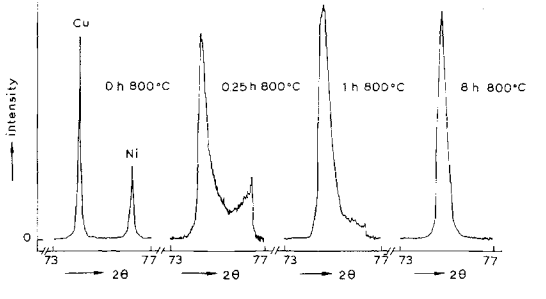

Figure 2 220 α_1 line profiles of an interdiffused Cu/Ni powder specimen for various annealing times at 800° C.

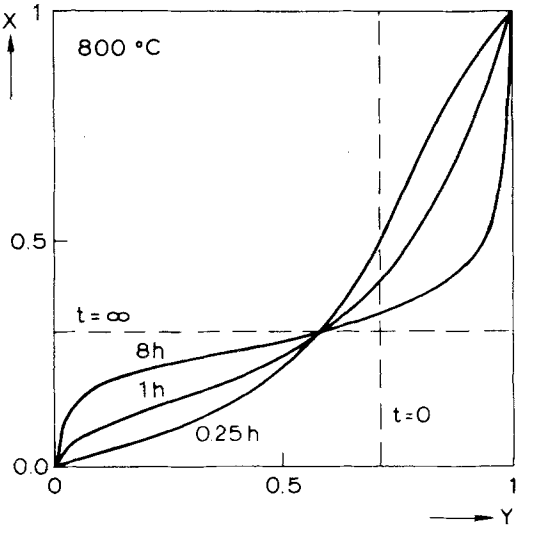

Figure 3 Concentration-effective penetration curves as calculated according to the method outlined in Section 3 from the line profiles of Fig. 2. x is the atomic fraction nickel and y is the effective penetration distance (Equation 2).

4. Results with the Rudman method

Fig. 2 shows α_1 line profiles of a Cu/Ni powder specimen for various stages of interdiffusion. In Fig. 3 the corresponding concentration-effective penetration curves are given (Equations 1 and 2).* The degree of interdiffusion F can be obtained by numerical integration of the concentration-effective penetration curves (Equation 3). The results are summarized in Fig. 4.

Adopting the concentric sphere model a Dt value can be assigned to each experimental F value (Fig. 1). In Fig. 5 the Dt values obtained are plotted versus t. If the concentric sphere model is ideally suited to describe interdiffusion in these powder specimens, straight lines should have been obtained, with slopes corresponding to the respective diffusion coefficients. Clearly this is not the case.

From Fig. 5 it is seen that at the start of homogenization diffusion is very fast. This effect was investigated by additional experiments at rather low temperatures, the results of which are gathered in Table I. Considering the insensitivity of F to changes in the model of diffusion (cf. Sections 3 and 6.2) Dt values may be assigned to the F values

*The behaviour of these curves in the immediate neighbourhood of $y = 0$ and $y = 1$ is not physically significant, because α_2 elimination [9] does not completely eliminate the broadening caused by the X-ray spectrum and the instrumental conditions. In principle deconvolution techniques [13] should give better results. However, in practice results obtained after deconvolution and after α_2 elimination show only small differences in the degree of interdiffusion [14].

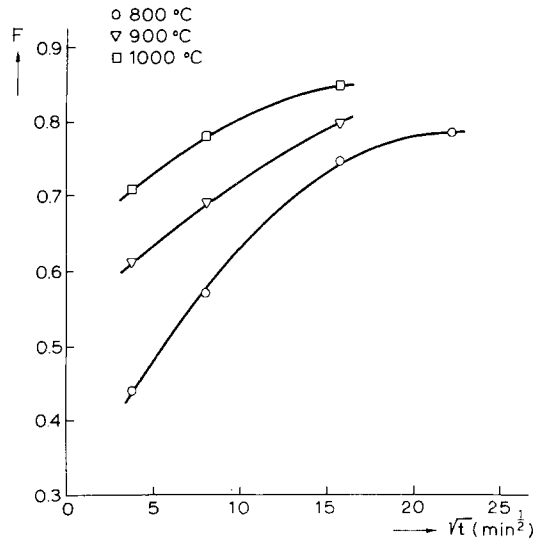

Figure 4 The observed variation of the degree of interdiffusion F as a function of the annealing time t for Cu/Ni powder specimens interdiffused at 800, 900 and 1000° C.

in the same way as before. Assuming an Arrhenius-type temperature dependence the activation energy of the fast diffusion process is estimated to be 12 kcal mol^{-1}. As compared with data on volume diffusion [15] this activation energy indicates surface diffusion [16]. At the contact places between the copper and nickel particles surface diffusion contributes significantly at the start of the homogenization at 800, 900 and 1000° C. The local character of this process is demonstrated by the α_1 line profile of the Cu/Ni powder specimen annealed at 634° C for 15 min. (Fig. 6). Apart from the nickel and copper peak two neighbouring maxima can be observed, which show that homogenization occurred locally not affecting the bulk of the copper and nickel particles.

TABLE I Results of the experiments at relatively low temperatures, t = time of diffusion, T = annealing temperature, F = degree of interdiffusion and D = diffusion coefficient.

t(min)	T(° C)	F	D(cm^2 sec^{-1}
15	634	0.41	2.0×10^{-11}
15	664	0.46	2.6×10^{-11}
15	694	0.49	3.0×10^{-11}

From Fig. 5 it is seen that at large homogenization times the apparent diffusion coefficients become small. According to Heckel *et al.* [1] this illustrates the effects of non-ideal mixing and non-uniform particle sizes. In Section 7 an approach on

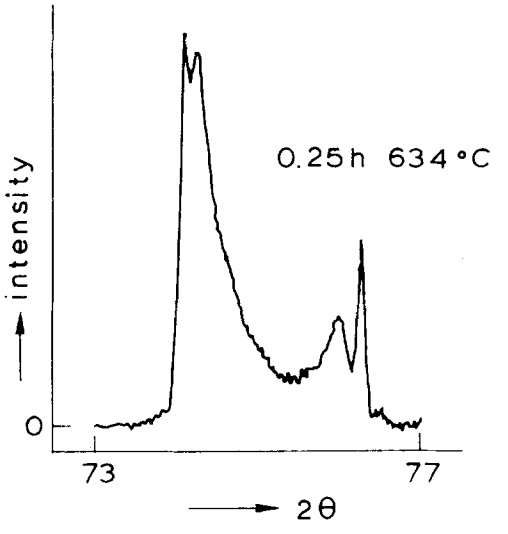

Figure 6 220 α_1 line profile taken from a Cu/Ni powder specimen annealed at 634° C for 15 min.

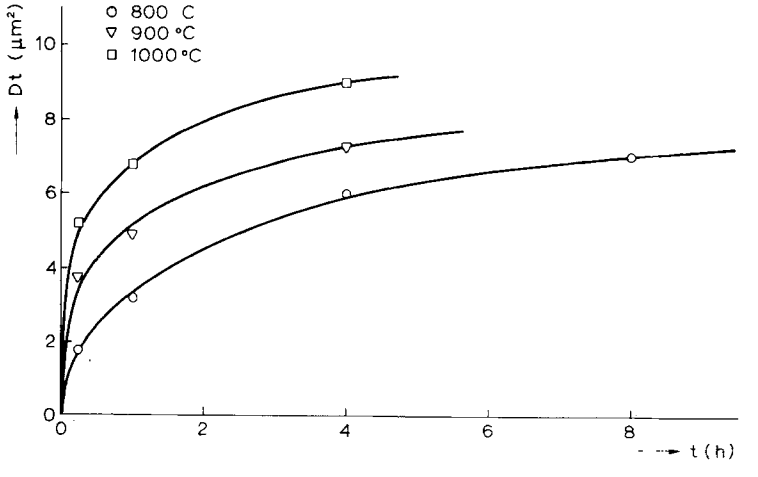

Figure 5 Graphs of Dt versus t; Dt values are calculated according to the concentric sphere model from Fig. 1. Note that straight lines should have been obtained, with slopes corresponding to the respective diffusion coefficients, if the concentric sphere model held.

the basis of an effective particle size will be presented to deal with this problem.

5. Line profile simulation method

Let us divide the radial concentration profile in the concentric sphere in segments (shells) corresponding to a constant change of concentration. Each segment k will diffract at a certain s ($= 2 \sin\theta/\lambda$) value, say s_k. We assume that all the segments give rise to a diffracted profile of the same shape. This implies that the structural broadening of a segment owing to its concentration variation is neglected as compared to the spectral and instrumental broadening. The intensity of the profile of segment k will be proportional to the amount of material of segment k. Then for the powder specimen the profile $i_k(s)$ of segment k can be written as

$$i_k(s) = C_2 \frac{1}{v_k^2} \frac{4}{3}\pi\{(R-r_{k-1})^3 - (R-r_k)^3\} f(s-s_k) \qquad (4)$$

where C_2 is a constant (including the absorption factor which is approximately constant), v_k is the average unit cell volume of segment k, R is the radius of the concentric sphere, the radii r_{k-1} and r_k enclose segment k ($k = 1, 2, \ldots$ and $r_0 = R$) and f describes the shape of the diffracted profile such that $f(0) = 1$.

The total line profile of the powder specimen will be the sum of the profiles of all segments. Dividing the intensities by the peak intensity I_0 of the major component before interdiffusion, the total line profile is given by

$$\frac{I(s)}{I_0} = \frac{v_B^2}{\{R^3 - (R-r_B)^3\}} \sum_k \frac{1}{v_k^2} \{(R-r_{k-1})^3 - (R-r_k)^3\} f(s-s_k) \qquad (5)$$

In order to obtain the shape function f the α_1 line profile of a standard nickel powder specimen was determined. The full width at half maximum was found to be 0.8×10^{-3} Å^{-1}. According to Edwards and Langford [17] the contribution of the spectral broadening to this width is (0.5 to 0.7) $\times$ 10^{-3} Å^{-1}. Hence the spectral broadening dominates over the broadening due to the instrumental conditions. It is generally accepted that the spectral α_1 component can be described by a Cauchy-function [18]. From the above we conclude that a reasonable approximation to the shape function

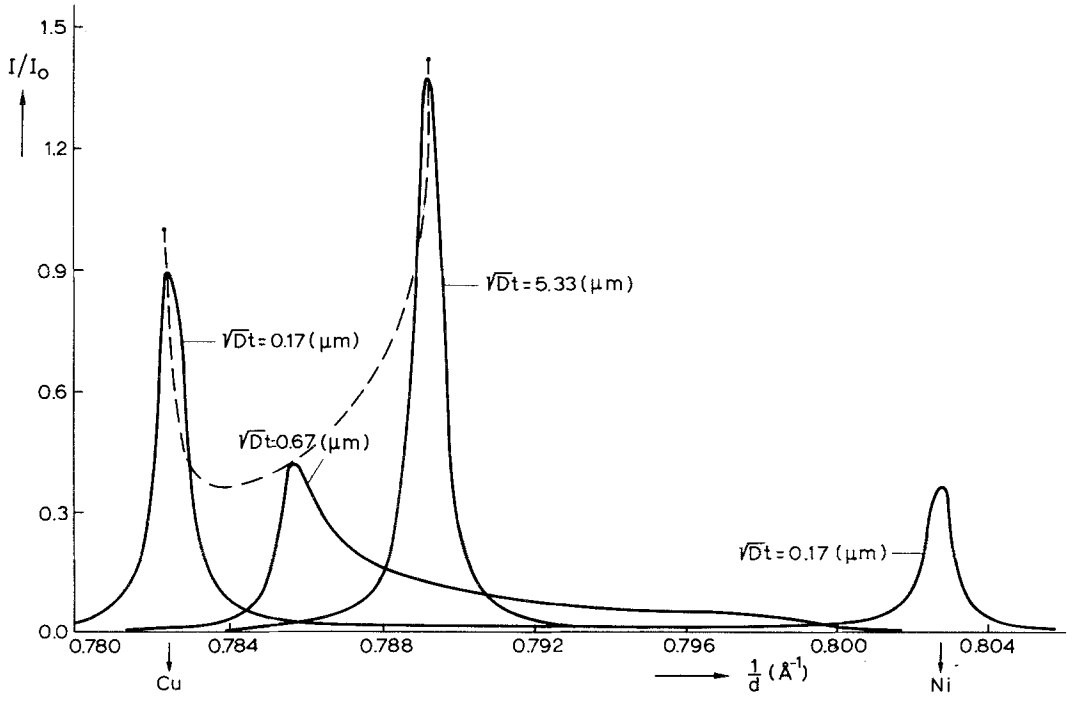

Figure 7 Computer simulations of 220 α_1 line profiles of Cu/Ni powder specimens for various stages of interdiffusion according to the concentric sphere model. The behaviour of the copper-side peak maximum on annealing is indicated by the dashed curve.

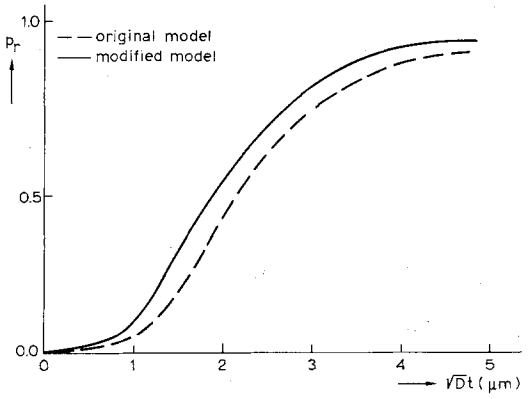

Figure 8 The relative peak position p_r as a function of $\sqrt{Dt}$ according to the original concentric sphere model and the modified one (cf. Section 6.2).

is given by a Cauchy-function having a full width at half maximum of 0.8×10^{-3} Å^{-1}.

Results of simulations of the 2 2 0 line profile of an interdiffused Cu/Ni powder specimen on the basis of Equation 5 are shown in Fig. 7 for various stages of interdiffusion (the corresponding concentration profiles were calculated according to the concentric sphere model).

We propose to characterize homogenization by the relative peak position p_r defined as

$$p_r = (p - p_0)/(p_\infty - p_0) \qquad (6)$$

where p is the actual peak position and p_0 and p_∞ correspond to the peak positions at the start and at the end of homogenization respectively. p_∞ can be calculated from the mean composition.

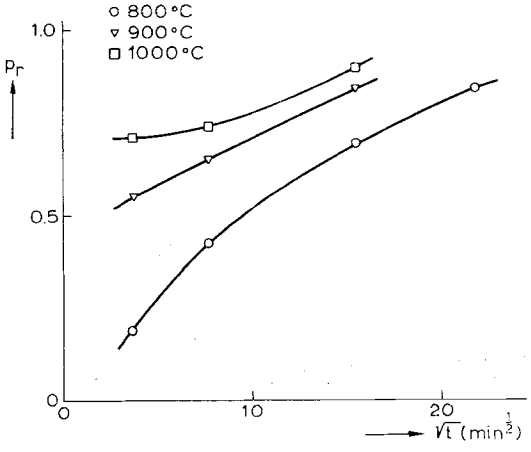

Figure 9 The observed variation of the relative peak position p_r as a function of the annealing time t for Cu/Ni powder specimens interdiffused at 800, 900 and 1000° C.

In our case (0.3 atomic fraction nickel) it is clear that the copper-side peak should be traced during interdiffusion: in Fig. 7 the behaviour of the copper-side peak maximum on annealing is also indicated (dashed curve). On the basis of the line profile simulations according to the concentric sphere model the relative peak position is plotted as a function of Dt in Fig. 8. This plot plays the same role in our method as Fig. 1 in the Rudman method: once the value of p_r is established the value of Dt is obtained according to the concentric sphere model. It is clear that the relative peak position is much easier as well as much faster to determine than the degree of interdiffusion (cf. Section 3).

6. Results with the line profile simulation method

6.1. Comparison with the Rudman method

Experimentally determined values for the relative peak position are presented as a function of annealing time and temperature in Fig. 9. Using Fig. 8 a Dt value can be assigned to each p_r value according to the concentric sphere model, from which graphs of Dt versus t (as given in Fig. 5 for the Rudman method) can be constructed. Then the same conclusions as obtained before can be reached by similar reasoning. Generally it can be said that the conclusions which are obtained by the Rudman method can also be provided by the line profile simulation method, which method is much simpler and faster to apply.

6.2. A modification to the concentric sphere model

Notwithstanding the above, differences in results exist between the Rudman method and the line profile simulation method: the dashed line in Fig. 10 represents the relation between the relative peak position p_r and the degree of interdiffusion F according to the concentric sphere model ($p_r \rightarrow Dt$ (Fig. 8); $Dt \rightarrow F$ (Fig. 1)). The experimental points are also indicated. The correspondence between experiment and the concentric sphere model is not very satisfactory, because all experimental points lie above the dashed curve.

Now we recall the fast surface diffusion process which occurs at the start of the homogenization at 800, 900 and 1000° C, as is shown in Section 4. The time required to establish local homogenization at the contact places between the copper and

nickel particles by surface diffusion may be neglected with respect to the total annealing times at these temperatures. It was assumed that an initial concentration profile in the concentric sphere model with a pre-alloyed shell at the copper/nickel interface at $t = 0$ might give a better description of the homogenization behaviour observed at these temperatures. This model has been worked out in the Appendix. For the present case additional assumptions were made: (i) Homogenization in the pre-alloyed shell was considered as completed. (ii) The thickness $(\Delta_1 + \Delta_2)$ of the pre-alloyed shell was estimated from the low temperature experiments reported in Section 4 by $(\Delta_1 + \Delta_2)^2 \simeq 2Dt \simeq 4\,\mu m^2$, where the radial dimensions Δ_1 and Δ_2 were taken as equal. The dependence of F on Dt according to this modified concentric sphere model is also plotted in Fig. 1. It follows that in the range of F values which covers all experiments (0.45 to 0.90), the differences in Dt values between the original concentric sphere model and the modified one are negligible. This illustrates the insensitivity of the degree of interdiffusion to deviations from the concentric sphere model, as mentioned in Section 3. The relative peak position is much more sensitive to such deviations as follows from Fig. 8. In Fig. 10 the relation between p_r and F for the modified concentric sphere model is also given (bold line). It can be seen that a good correspondence exists between the predictions of the modified concentric sphere model and the experiments.

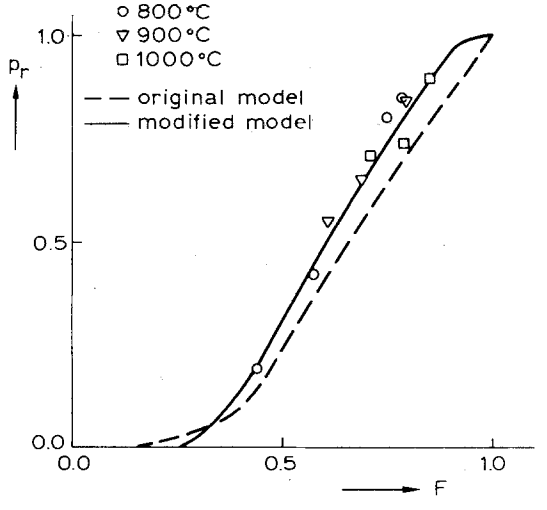

Figure 10 The relative peak position p_r as a function of the degree of interdiffusion F for the original concentric sphere model (dashed curve) and the modified one (bold curve). The experimental points are also shown.

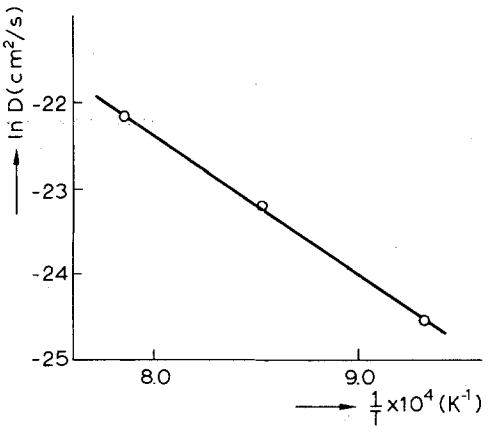

Figure 11 Ln D versus $1/T$. Only the ratios of the diffusion coefficients are physically significant. The given values of the diffusion coefficients result from the definition of $a_e = 1$ (cf. Fig. 12). This does not affect the determination of the activation energy.

7. Activation energy and diffusion mechanism

Without knowing the actual diffusion geometry in the powder specimens employed it is possible to determine the activation energy of the diffusion process. Assuming one diffusion mechanism to be dominant, it is recognized that equal values of the relative peak position at different temperatures imply identical stages of homogenization in the powder specimen. Hence the ratios of the diffusion coefficients at these temperatures are given by the ratios of the annealing times, which can be obtained by interpolation in Fig. 9. From an Arrhenius-plot the activation energy can be obtained (Fig. 11)

$$Q = 32\,\text{kcal mol}^{-1}$$

As compared with data on volume diffusion [15] this activation energy indicates grain boundary diffusion [16]. This agrees with previous results on polycrystalline Cu/Ni specimens [5, 19]. The result contradicts the statement of Heckel [1, 6] who claims volume diffusion to be dominant; however no activation energy was reported.

In Section 4 the decrease in the apparent diffusion coefficients at large annealing times was noted (cf. Fig. 5). This was attributed to deviations in the powder specimen from the diffusion geometry adopted: larger diffusion distances (e.g. contiguous nickel particles) become dominant at longer diffusion times causing a progressive decrease of the rate of homogenization. This problem can be dealt with as follows.

In the case of a concentration independent diffusion coefficient Fick's second law can be solved for concentric sphere geometries in terms of the dimensionless parameter Dt/a^2, where a is the radius of the nucleus (= nickel particle). Because at one annealing temperature the diffusion coefficient should be constant, the homogenization of non-ideally mixed powders with non-uniform particle sizes can be described by varying the radius a on annealing to accord with the (modified) concentric sphere model. We now introduce an effective particle size a_e, as suggested by Heckel [6]. After choosing a reference particle size a_r, it is possible for experiments with different annealing times at the same temperature to calculate the effective particle size $a_e = a/a_r$ in such a way that D remains constant. The results at different annealing temperatures can be related, because equal values of the relative peak position point to identical stages of homogenization. This implies that at the same values of the relative peak position one single effective particle size operates. In this way effective particle sizes at different temperatures can be brought into accordance, see Fig. 12. It is seen that all effective particle sizes observed lie approximately on a single curve. This illustrates that one single diffusion mechanism is dominant in the temperature range applied, as was assumed for the determination of the activation energy.

Appendix

The modified concentric sphere model

Metallographic evidence [5, 6] indicated that the geometry in binary powder specimens may be described by the concentric sphere geometry. A perfect distribution of the minor component A (in our case nickel) in the matrix of the major component B (in our case copper) is assumed. Then a concentric sphere with A and B constituting the sphere and the shell respectively may be a reasonable approximation of reality.

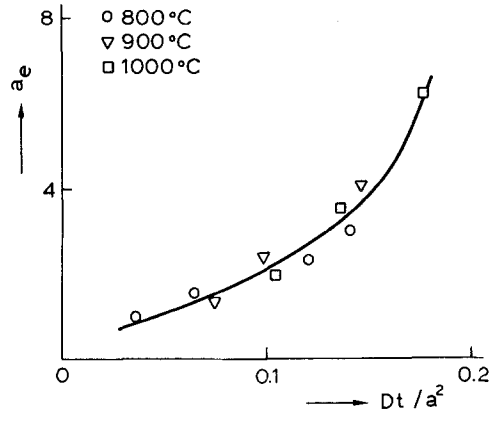

Figure 12 The effective particles size a_e as a function of Dt/a^2, where a is the radius of the nucleus. The effective particle size was arbitrarily set equal to 1 for the experiment at 800° C with 15 min annealing time.

A general solution to Fick's second law with a concentration independent diffusion coefficient for diffusion in a sphere with impermeable surface was given by Crank (Equation 6.47 in [20]). In our case the concentration distribution $f(r)$ at $t = 0$ is given by

$$0 < r < a \quad f(r) = 1 \quad \text{and} \quad a < r < b \quad f(r) = 0 \qquad \text{(case 1)}$$

where a and b are the radii of the nucleus and the concentric sphere respectively.

In Section 6.2 it is shown that a more realistic description of the homogenization behaviour is obtained if a pre-alloyed shell at the A/B interface is thought to be present at $t = 0$. To a first approximation it is assumed that homogenization in the pre-alloyed shell leads to $c_L = 0.5$ (better approximations cause second order corrections). Then for the initial concentration distribution $f(r)$ it follows

$$0 < r < a - \Delta_1 \quad f(r) = 1;$$

$$a - \Delta_1 < r < a + \Delta_2 \quad f(r) = 0.5$$

and

$$a + \Delta_2 < r < b \quad f(r) = 0, \qquad \text{(case 2)}$$

where $\Delta_1 + \Delta_2$ is the radial dimension of the pre-alloyed shell and $c_L = \{a^3 - (a - \Delta_1)^3\}/\{(a + \Delta_2)^3 - (a - \Delta_1)^3\}$.

Evaluation of the integrals in Crank's formula yields for case 2

$$c(r) = \frac{a^3}{b^3} + \frac{2}{br} \sum_{n=1}^{\infty} \exp(-Dt\,\alpha_n^2) \frac{\sin \alpha_n r}{\sin^2 \alpha_n b}$$

$$\times \frac{1}{2\alpha_n} \Bigg\{ (a-\Delta_1)\cos \alpha_n (a-\Delta_1)$$

$$+ (a+\Delta_2)\cos \alpha_n (a+\Delta_2)$$

$$- \frac{\sin \alpha_n (a-\Delta_1)}{\alpha_n} - \frac{\sin \alpha_n (a+\Delta_2)}{\alpha_n} \Bigg\} \qquad \text{(A1)}$$

where $c(r)$ is the volume fraction of material A and α_n is the nth positive root of the transcendental equation $b\alpha_n \cot b\alpha_n = 1$.

The quantity of material m_t which has crossed the interface after a given diffusion time t and the quantity of material m_∞ which will cross in infinite time follow from

$$m_t = 4\pi\int_0^{a/b}(1-c)\left(\frac{r}{b}\right)^2 \mathrm{d}\left(\frac{r}{b}\right) + 4\pi\int_{a/b}^{1} c\left(\frac{r}{b}\right)^2 \mathrm{d}\left(\frac{r}{b}\right)$$

$$m_\infty = \frac{8\pi a^3}{3b^3}\left(1-\frac{a^3}{b^3}\right)$$

The degree of interdiffusion $F = m_t/m_\infty$ can be calculated from

$$F = 1 - \frac{16\pi}{b^4 m_\infty}\sum_{n=1}^{\infty}\exp(-Dt\,\alpha_n^2)\frac{1}{\sin^2\alpha_n b} \times \frac{1}{2\alpha_n^2}\left\{(a-\Delta_1)\cos\alpha_n(a-\Delta_2)\cos\alpha_n(a+\Delta_2) - \frac{\sin\alpha_n(a-\Delta_1)}{\alpha_n} - \frac{\sin\alpha_n(a+\Delta_2)}{\alpha_n}\right\} \times \left\{a\cos\alpha_n a - \frac{\sin\alpha_n a}{\alpha_n}\right\} \quad \text{(A2)}$$

The formulae for the original concentric sphere model (case 1) follow immediately from the formulae for the modified concentric sphere model (case 2) if $\Delta_1 \to 0$ and $\Delta_2 \to 0$ in Equations A1 and A2.

The dependence of F on Dt, as calculated from Equation A2, is plotted for both models in Fig. 1.

Acknowledgements

We are indebted to Professor B. Okkerse and Dr F. W. Schapink for reading the manuscript critically. Financial support of the Stichting voor Fundamenteel Onderzoek der Materie (FOM) is gratefully acknowledged.

References

1. R. W. HECKEL and M. BALASUBRAMANIAM, *Met. Trans.* **2** (1971) 379.
2. C. R. HOUSKA, *J. Appl. Phys.* **41** (1970) 69.
3. E. J. MITTEMEIJER and R. DELHEZ, *ibid.* 47 (1976) 1702
4. P. S. RUDMAN, *Acta Cryst.* **13** (1960) 905.
5. B. FISHER and P. S. RUDMAN, *J. Appl. Phys.* **32** (1961) 1604.
6. R. W. HECKEL, *Trans. ASM* 57 (1964) 443.
7. D. Y. F. LAI, Proceedings of the International Conference of the American Society for Metals (Metals Park, Ohio, 1964) p. 269.
8. A. J. C. WILSON, "Elements of X-ray Crystallography" (Addison–Wesley, Reading, Massachusetts, 1970) p. 34.
9. R. DELHEZ and E. J. MITTEMEIJER, *J. Appl. Cryst.* 8 (1975) 609.
10. R. DELHEZ, E. J. MITTEMEIJER, Th. H. de KEIJSER and H. C. F. ROZENDAAL, *J. Phys. E.* **10** (1977) 784.
11. International Tables for X-ray Crystallography Vols. III and IV, published for the International Union of Crystallography (The Kynoch Press, Birmingham, 1962, 1974).
12. B. E. WARREN, "X-ray Diffraction" (Addison–Wesley, Reading Massachusetts, 1969) p. 49.
13. A. R. STOKES, *Proc. Phys. Soc.* **61** (1948) 382.
14. E. A. van den BERGEN, R. DELHEZ and E. J. MITTEMEIJER, *Phys. Stat. Sol. (a)* **44** (1977) 517.
15. Diffusion Data **2** (1968) 271 (for example).
16. J. ASKILL, "Tracer Diffusion Data for Metals, Alloys and Simple Oxides" (Plenum Press, New York, 1970) p. 11.
17. H. J. EDWARDS and J. I. LANGFORD, *J. Appl. Cryst.* 4 (1971) 43.
18. H. P. KLUG and L. E. ALEXANDER, "X-ray Diffraction Procedures for Polycrystalline and Amorphous Materials", 2nd edition (John Wiley, New York, 1974) p. 297.
19. G. O. TRONSDAL and H. SORUM, *Phys. Stat. Sol.* **4** (1964) 493.
20. J. CRANK, "The Mathematics of Diffusion" (Clarendon Press, Oxford, 1956) p. 92.

Received 16 September and accepted 1 November 1977.